Effect of Ni–Co codoping on structure and electrical properties of multiferroic $BiFeO_3$ nanoparticles

Sk Mazaffar Hossain[1], Ayan Mukherjee[1], Soumen Basu[1], Mrinal Pal[2]

[1]*Department of Physics, National Institute of Technology, Durgapur 713209, West Bengal, India*
[2]*CSIR-Central Mechanical Engineering Research Institute, Durgapur 713209, West Bengal, India*
E-mail: m_pal@cmeri.res.in

Published in Micro & Nano Letters; Received on 13th February 2013; Accepted on 22nd May 2013

Ni and Co doped nanocrystalline $BiFeO_3$ (BFO) have been prepared using a facile sol–gel technique. The effects of codoping on the crystal structure, morphology and electrical properties are investigated. X-ray diffraction and high-resolution transmission electron microscopy studies confirm the phase purity and growth of BFO nanoparticles. The heat-flow measurement using a differential thermal analyser shows an endothermic peak between 1070 and 1100 K representing ferroelectric to paraelectric phase transition. A systematic electrical conductivity study of these nanoparticles delineates that resistivity increases for doped BFO samples which is very much desirable for device applications of multiferroics.

1. Introduction: Multiferroic materials possess the properties of ferromagnetism, ferroelectricity and even ferroelasticity simultaneously in single phase because of the coupling between ferroelectric and magnetic orders. They have attracted much attention in recent years, because of their potential for new devices starting from information storage to sensor applications [1–4]. The important multiferroic systems studied so far include $BiFeO_3$ (BFO), $BiMnO_3$ and $ReMnO_3$ (Re = Y, Ho-Lu). Among them, BFO, which crystallises in a distorted rhombohedral structure (space group R-3c), is unique, as the material exhibits both ferroelectric and antiferromagnetic (AFM) order simultaneously above room temperature [5]. However, pure BFO has a serious problem of high leakage current resulting from charge defect which prevents it from gaining good ferroelectricity.

Recently, different synthesis processes have been adopted to obtain single phase BFO with improved multiferroic properties. Up to now, reported work involving the synthesis of single phase BFO having enhanced multiferroic properties has been mainly based on two different techniques: suitable transition elements/rare earth ion doping and controlling the size by optimising the preparation parameters. To improve the electrical properties of BFO, several research groups have attempted to dope +3 valence lanthanide ions [La^{3+}, Nd^{3+} or Sm^{3+}] at the A site of BFO (ABO_3) [6–8]. The doping has resulted in reduction of leakage current density and improvement in the ferroelectric properties of BFO to some extent. However, to the best of our knowledge, there is hardly any report about the detailed mechanism of electrical conduction so far. Keeping in view the importance of BFO, it seems to be interesting to investigate the detailed conductivity mechanism. Here, we report the synthesis and electrical transport properties of cobalt and nickel ion codoped BFO nanoparticles.

2. Experimental: We have prepared pure and doped BFO by a facile sol–gel technique using metal nitrates as precursors. In the first step, three precursor solutions were prepared by dissolving a weighted amount of $Bi(NO_3)_3{\cdot}5H_2O$, $Fe(NO_3)_3{\cdot}9H_2O$ and $Ni(NO_3)_3/Co(NO_3)_3$ in 10 ml of distilled water under continuous stirring. HNO_3 was used to maintain the pH of the solution to 2. In the next step, maleic acid (0.03 mol) was dissolved in distilled water (30 ml) in a separate beaker. Metal nitrate precursor solutions were added to the maleic acid under constant stirring. Polyethylene glycol (PEG) in a molar ratio to maleic acid of 1:1 was finally added to the solution as a polymerising agent. The solution was evaporated to obtain a dry polyester precursor powder. Finally the grinded powders were calcined in air at 873 K for 2 h with a heating rate of 400 K/h.

Thermal analysis was performed using a differential thermal analyser (DTA) of NETZSCH (STA449 F1-Jupiter) to study the phase transition in synthesised $BiFe_{1-x}(Ni, Co)_xO_3$. X-ray diffraction studies of the samples were carried out in a Panalytical X-ray diffractometer (XRD) with CuK_α radiation. Microstructural analysis for the samples was carried out using a high-resolution transmission electron microscope (HRTEM) of JEOL (model 2010) operated at 200 kV. For the transmission electron microscope (TEM) study the samples were ground in an agate mortar, dispersed in ethanol by sonication and cast one drop on a copper grid coated with a graphite foil. A custom designed sample holder with a coaxial cable attached to an LCR meter has been used for electrical measurement. Samples were electroded using silver paste for electrical measurement in the frequency range between 50 kHz and 600 MHz.

3. Result and discussions: XRD data were analysed to identify the crystal structure and also to check the presence of various phases/impurities in the samples. The powder diffraction patterns of pure and Ni, Co and codoped BFO samples are shown in Fig. 1.

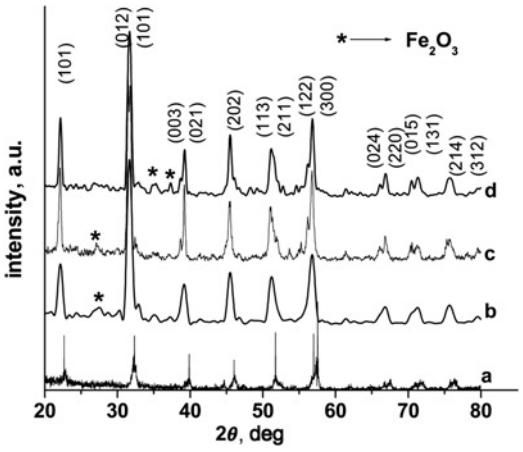

Figure 1 *XRD patterns*
a Pure $BiFeO_3$
b $BiFe_{0.9}Co_{0.1}O_3$
c $BiFe_{0.9}Ni_{0.1}O_3$
d $BiFe_{0.9}Co_{0.05}Ni_{0.05}O_3$ nanoparticles

doi: 10.1049/mnl.2013.0078

Comparison of the experimental data with the JCPDS file (Card No. 014 0181) shows that all the reflections correspond to the BFO phase. From the XRD analysis, it is very clear that all the samples exhibit single phase polycrystalline rhombohedral perovskite crystal. This observation reveals that the dopants' concentration level remains below the solubility limit of the parent compound.

The detail microstructure of BFO nanoparticles was investigated using TEM to understand the effect of doping. Fig. 2*a* shows Co–Ni codoped bismuth ferrite ($BiFe_{0.9}Co_{0.05}Ni_{0.05}O_3$) nanoparticles. The micrograph clearly demonstrates that the nanoparticles are agglomerated a little bit and not exactly spherical in shape. Average particle size has been estimated by using standard log-normal distribution, and found to be 40 nm. The atomic structures were characterised from the HRTEM image which is shown in Fig. 2*b*. The HRTEM image shows good crystallinity with clear resolution of lattice fringes. The interplanar distance of fringes was measured to be 2.28 Å, which corresponds to the (012) planes of BFO. Phase characterisation has also been performed from the selected area diffraction patterns of the TEM presented in Fig. 2*c*. We observe that all the diffraction plane match well with BFO, which reconfirm the purity of the prepared samples.

DTA analysis of all the samples was performed to estimate ferroelectric phase transition temperatures. Fig. 3 shows the DTA pattern

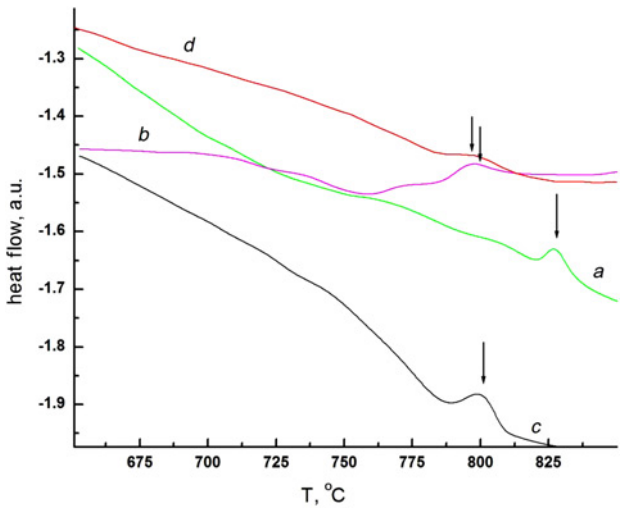

Figure 3 *DTA patterns*
a Pure $BiFe_3$
b $BiFe_{0.9}Co_{0.1}O_3$
c $BiFe_{0.9}Ni_{0.1}O_3$
d $BiFe_{0.9}Co_{0.05}Ni_{0.05}O_3$ nanoparticles

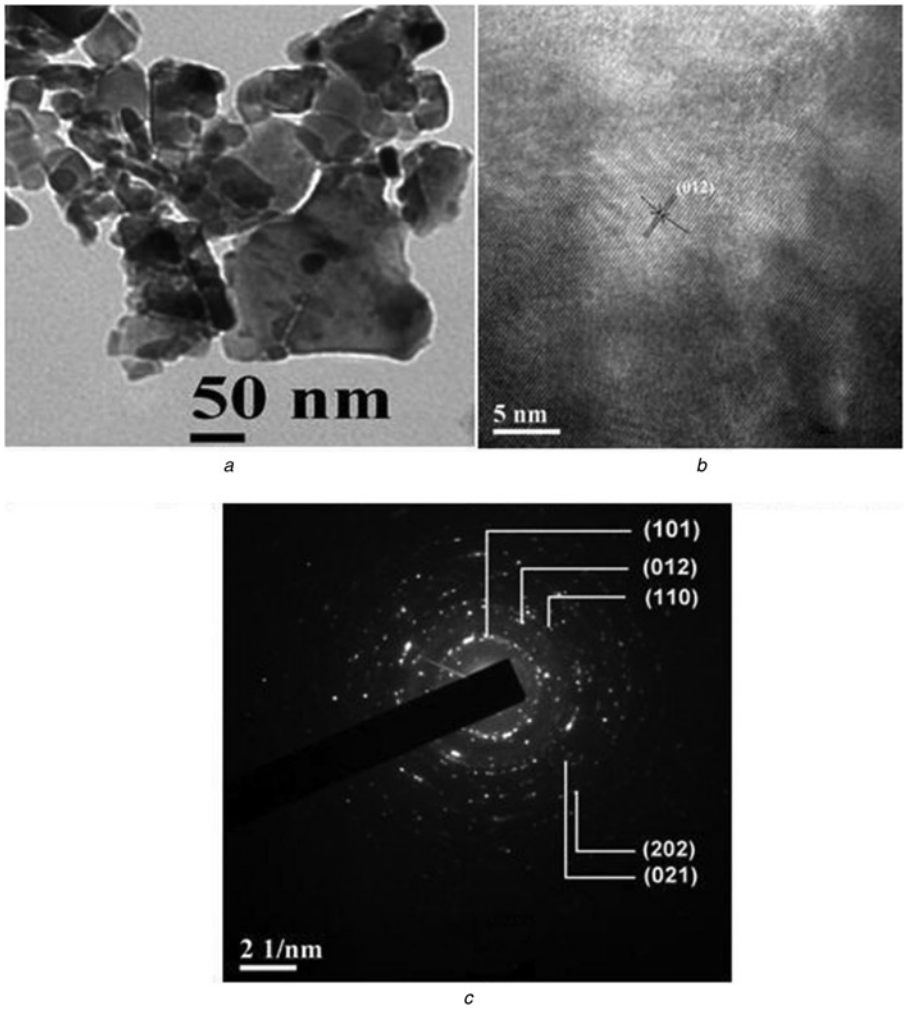

Figure 2 *Transmission electron micrograph of Co–Ni codoped ($BiFe_{0.9}Co_{0.05}Ni_{0.05}O_3$) nanoparticles*
a Particle size distribution
b High resolution image of $BiFe_{0.9}Co_{0.05}Ni_{0.05}O_3$ nanoparticles
c SAED pattern taken from a portion of (Fig. 2*a*)

observed for different samples heated at a constant rate of 10 K/min up to 1173 K (900°C) in nitrogen atmosphere. To delineate the effect of different transition metal ion doping on ferroelectric phase transition we have shown enlarged views in the temperature range 1053–1143 K (780–870°C). A distinct endothermic peak between 1070 and 1100 K (797–827°C) in the heat flow against temperature curve is observed. The endothermic peaks shown in Fig. 3 are because of the ferroelectric transition of the bismuth ferrite samples, which is consistent with the previous report [8]. Also, similar phase transition was observed from variation of the dielectric constant with temperature at 1120 K (847°C) [9]. The observed phase transition temperatures are summarised in Table 1. It was observed that phase transition temperatures decrease when doped with transition metal Co/Ni in comparison to the pure sample, which can be attributed to the decrease of particle size because of doping.

The dc electrical transport properties of doped BFO have been measured in the temperature range 298–523 K. Fig. 4 shows the variation of dc resistivity with temperature. All the samples behave like semiconducting materials, that is, their resistivity decreases with the rise in temperature. The dc activation energy was estimated by using the Arrhenius relation from the slope of the graphs and is summarised in Table 1. It is evident from the Figure that with increasing content of dopants, there is an increase in the resistivity of the samples by a significant amount. It was found that among all the samples, codoped (both Co and Ni) samples exhibit the highest resistivity. The increase of resistivity implies a decrease of leakage current in BFO, which is very much essential for device applications. It is well known that high leakage current densities in pure or doped BFO originate mainly from vacancies of Bi or oxygen. Oxygen vacancy comes from Bi volatility and transition from Fe^{3+} to Fe^{2+}. Therefore we can increase the resistivity and in turn decrease the leakage current density in the doped samples to decrease the number of these vacancies.

Table 1 Ferroelectric transition temperature and dc activation energy for different samples

Name of sample	Ferroelectric transition temperature, °C	Activation energy, eV
pure $BiFeO_3$	827	1.1323
$BiFe_{0.9}Co_{0.1}O_3$	797	0.8161
$BiFe_{0.9}Ni_{0.1}O_3$	800	0.82004
$BiFe_{0.9}Co_{0.05}Ni_{0.05}O_3$	798	0.68833

The ac conductivity of BFO samples has been measured in the temperature range $298 \leq T \leq 523$ K and in the frequency range 20 Hz to 1 MHz. At lower frequency range, the conductivity remains unchanged but the changes become predominant at higher frequency for a particular temperature. In general many amorphous semiconductors or disordered systems have dc conductivity contribution (σ_{dc}) besides ac conductivity. This may be the reason behind the frequency independence of conductivity at the lower frequency region. Total conductivity at a particular temperature over a wide range of frequency obeys a power law with frequency, which can be expressed as [10–13]

$$\sigma'(f) = \sigma_{dc} + \sigma_{ac}(f) = \sigma_{dc} + \alpha f^{S} \quad (1)$$

where σ_{dc} is dc conductivity, α is the temperature dependent constant and the frequency exponent 's' ≤ 1. The frequency dependent contribution can be calculated by subtracting the dc contribution from total conductivity.

's' can be estimated from the plot of $\ln[\sigma_{ac}(\omega)]$ with $\ln[\omega]$. The variation of 's' with temperature is shown in Fig. 5. A gradual decrease of 's' with increasing temperature is observed. In general, the nature of the conduction process of the disordered system is governed by two physical processes such as correlated barrier hopping (CBH) [11] and quantum mechanical tunnelling (electron tunnelling [12], small polaron tunnelling [13] and large polaron tunnelling [14]). The variations of 's' with temperature for different conduction processes are different. Observing the nature of variation of 's' the exact nature of the charge transport mechanism can be predicted. The frequency exponent 's' becomes independent of temperature in electron tunnelling, whereas it increases with increasing temperature in the case of small polaron tunnelling and increases at first and then decreases with decreasing temperature according to large polaron tunnelling. According to the CBH model, the value of 's' only decreases gradually with temperature. The nature of the variation of 's' in the present investigation suggests that the CBH model is suitable for explaining the experimental data. According to this model, the charge carriers hop between the sites over the potential barrier separating them and the frequency

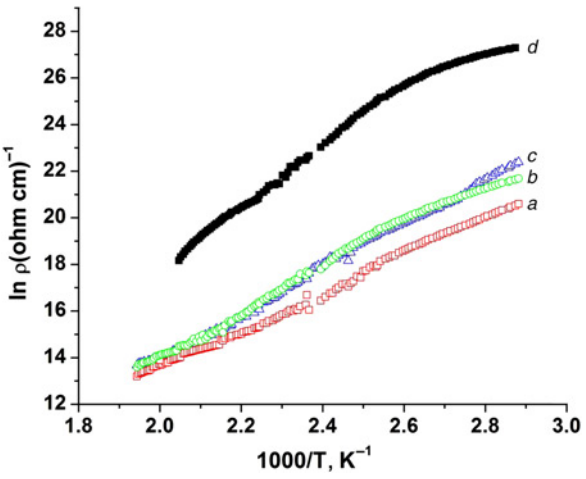

Figure 4 *Temperature dependence of dc conductivity of different doped and undoped Bi-ferrite samples*
a Pure $BiFeO_3$
b $BiFe_{0.9}Co_{0.1}O_3$
c $BiFe_{0.9}Ni_{0.1}O_3$
d $BiFe_{0.9}Co_{0.05}Ni_{0.05}O_3$

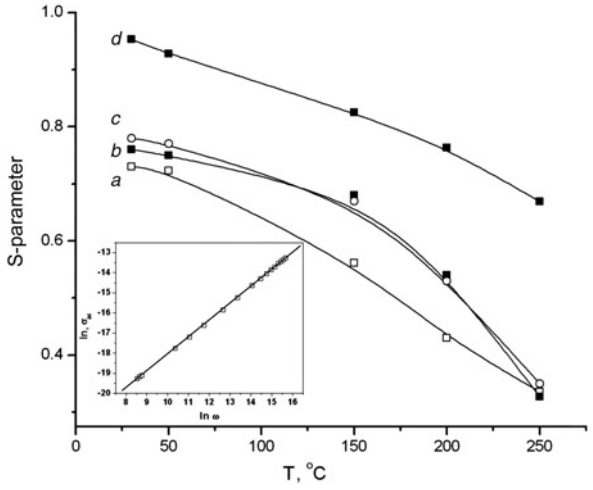

Figure 5 *Variation of S-parameter with temperature*
a Pure $BiFeO_3$
b $BiFe_{0.9}Co_{0.1}O_3$
c $BiFe_{0.9}Co_{0.05}Ni_{0.05}O_3$
d $BiFe_{0.9}Ni_{0.1}O_3$, inset shows ac conductivity variation with frequency of $BiFe_{0.9}Co_{0.05}Ni_{0.05}O_3$ sample at 323 K (50°C)

doi: 10.1049/mnl.2013.0078

Table 2 Effective barrier height and relaxation time for different samples

Name of sample	Effective barrier height, eV	Relaxation time, s
$BiFeO_3$	1.7	3.53×10^{-18}
$BiFe_{0.9}Co_{0.1}O_3$	1.1	0.77×10^{-13}
$BiFe_{0.9}Ni_{0.1}O_3$	1.4	5.25×10^{-13}
$BiFe_{0.9}Co_{0.05}Ni_{0.05}O_3$	1.5	1.3×10^{-13}

exponent 's' can be expressed as [11]

$$S = 1 - \frac{6k_BT}{W_H - k_BT\ln\left(1/\omega\tau_o\right)} \tag{2}$$

where k_B, W_H, ω and τ_o are the Boltzmann constant, effective barrier height, angular frequency and characteristic relaxation time, respectively.

Thus, the experimental data have been analysed with (2) as a function of temperature keeping W_H and $\omega\tau_o$ as a fitting parameter. The points indicate the experimental data and solid lines give the theoretical best fit obtained from (2) for different samples. The values of W_H and τ_o have been calculated at a fixed frequency of 10 kHz and are listed in Table 2. The trend of variation of 's' with temperature suggests that the charge transport mechanism of the investigated samples can be explained by the CBH model.

4. Conclusion: A facile synthesis method has been employed to prepare Co/Ni-doped $BiFeO_3$ nanoparticles. We have investigated the effects of codoping (Co, Ni) on the structure, morphology and electrical properties of these nanocomposites. Doping increases the electrical resistivity of nanocrystalline BFO by approximately five orders of magnitude for the codoped sample which is quite high and interesting too. The ac conductivity variation as a function of frequency in the range (20 Hz to 1 MHz) and temperature (range 298–523 K) was explained on the basis of the CBH conduction mechanism. The enhancement of resistivity could be favourable for device applications in future.

5. Acknowledgments: The authors acknowledge financial support from the BRNS (project no. 2011/37P/14/BRNS), the Department of Atomic Energy (DAE), and the Government of India. A. Mukherjee thanks the Department of Science and Technology (DST) (SR/FTP/PS-66/2008), Government of India, for providing his fellowship.

6 References

[1] Ryu J., Priya S., Uchino K., Kim H.E.: 'Magnetoelectric effect in composites of magnetostrictive and piezoelectric materials', *J. Electroceram.*, 2002, **8**, pp. 107–120

[2] Wang J., Neaton J.B., Zheng H., *ET AL.*: 'Epitaxial $BiFeO_3$ multiferroic thin film heterostructures', *Science*, 2003, **14**, pp. 1719–1722

[3] Nuraje N., Dang X., Qi J., Allen M.A., Lei Y., Belcher A.M.: 'Biotemplated synthesis of Perovskite nanomaterials for solar energy conversion', *Adv. Mater.*, 2012, **24**, (21), pp. 2885–2889

[4] Kanai T., Ohkoshi S.I., Nakajima A., Watanabe T., Imoto K.H.: 'A ferroelectric ferromagnet composed of $(PLZT)_x(BiFeO3)_{1-x}$ solid solution', *Adv. Mater.*, 2001, **13**, (7), pp. 487–490

[5] Zhang S.T., Zhang Y., Lu M.H., *ET AL.*: 'Substitution-induced phase transition and enhanced multiferroic properties of $Bi_{1-x}La_xFeO_3$ ceramics', *Appl. Phys. Lett.*, 2006, **88**, (16), pp. 162901–162903

[6] MacDougall G.J., Christen H.M., Siemons W., *ET AL.*: 'Antiferromagnetic transitions in tetragonal-like $BiFeO_3$', *Phys. Rev. B*, 2012, **85**, (10), pp. 100406 (R)–100410

[7] Yuan G.L., Wing Or.S.: 'Multiferroicity in polarized single-phase$Bi_{0.875}Sm_{0.125}FeO_3$ ceramics', *J. Appl. Phys.*, 2006, **100**, (2), pp. 024109–024113

[8] Singh S.K., Ishiwara H.: 'Doping effect of rare-earth ions on electrical properties of $BiFeO_3$ thin films fabricated by chemical solution deposition', *Jpn. J. Appl. Phys.*, 2006, **45**, pp. 3194–3197

[9] Lu J., Gunter A., Schrette F., *ET AL.*: 'On the room temperature multiferroic $BiFeO_3$: magnetic, dielectric and thermal properties', *Eur. Phys. J. B*, 2010, **75**, pp. 451–460

[10] Chakrabarti K., Das K., Sarkar B., De S.K.: 'Magnetic and dielectric properties of Eu-doped $BiFeO_3$ nanoparticles by acetic acid-assisted sol-gel method', *J. Appl. Phys.*, 2011, **110**, (10), pp. 103905–103914

[11] Mott N.F., Davis E.: 'Electronic process in noncrystalline materials' (Clarendon, Oxford, 1979, 2nd edn)

[12] Elliott S.R.: 'Ac conduction in amorphous chalcogenide and pnictide semiconductors', *Adv. Phys.*, 1987, **36**, (2), pp. 135–217

[13] Long A.R.: 'Frequency-dependent loss in amorphous semiconductors', *Adv. Phys.*, 1982, **31**, (5), pp. 553–637

[14] Efros A.L.: 'On the theory of ac conduction in amorphous semiconductors and chalcogenide glasses', *Philos. Mag. B*, 1981, **43**, (5), pp. 829–838